

Construction of Chiral, Helical Nanoparticle Superstructures: Progress and Prospects

Soumitra Mokashi-Punekar, Yicheng Zhou, Sydney C. Brooks, and Nathaniel L. Rosi*

Chiral nanoparticle (NP) superstructures, in which discrete NPs are assembled into chiral architectures, represent an exciting and growing class of nanomaterials. Their enantiospecific properties make them promising candidates for a variety of potential applications. Helical NP superstructures are a rapidly expanding subclass of chiral nanomaterials in which NPs are arranged in three dimensions about a screw axis. Their intrinsic asymmetry gives rise to a variety of interesting properties, including plasmonic chiroptical activity in the visible spectrum, and they hold immense promise as chiroptical sensors and as components of optical metamaterials. Herein, a concise history of the foundational conceptual advances that helped define the field of chiral nanomaterials is provided, and some of the major achievements in the development of helical nanomaterials are highlighted. Next, the key methodologies employed to construct these materials are discussed, and specific merits that are offered by each assembly methodology are identified, as well as their potential disadvantages. Finally, some specific examples of the emerging applications of these materials are discussed and some areas of future development and research focus are proposed.

Chiral objects are defined as non-superimposable conformations that are mirror images of each other, much like a pair of left and right hands. In fact, the word “chiral” derives from the Greek word “ $\chi\epsilon\iota\rho$ ” (kheir), which translates to “hand.” Most biomolecules exist in only one particular conformation. For example, amino acids within large protein and peptide molecules are exclusively in the L-form (left-handed). It has long been considered that the phenomenon of homochirality (predominant occurrence of one conformation) could be linked to the origin of life.^[1] These phenomena have inspired chemists and biologists to isolate, synthesize, and study the properties of chiral molecules.

Research interest in chiral nanostructures has escalated rapidly since the early 2000s due to visionary reports that either predicted or demonstrated the potential applications of these materials.^[2,3] In 2004, Pendry predicted that chiral metamaterials could be used to achieve negative refraction

1. Introduction and Background


The essence of chemistry lies in building and transforming matter, atom by atom and molecule by molecule. The sequence and positions of atoms within molecules, the disposition of molecules and other chemical species in 3D space, their specific interactions—these determine the properties and functions of matter that underpin the bountiful complexity of life and nature. Chiral molecules and materials are quintessential, perhaps nonpareil, manifestations of chemistry and their precise construction from achiral building blocks is a continuing grand challenge in synthetic chemistry and materials science.

(Figure 1).^[2] Following this seminal work, others demonstrated that such materials lead to circular dichroism (CD),^[4] negative phase velocities,^[5] and intense gyrotropy,^[6] generating significant excitement within this emerging field. These properties can be harnessed to realize optical materials including “perfect lenses,”^[7] circular polarizers,^[3] chiroptical sensors,^[8] and negative refractive index materials.^[9,10] In addition to these optical applications, chiral metallic nanostructures have been used for detection of biomolecular disease precursors,^[11] chiral catalysis,^[12] and chiral separations.^[13]

Many of the promising applications of chiral metallic nanostructures arise in part from their plasmonic chiroptical activity. At the nanoscale, individual metallic particles exhibit unique properties due to their high surface to volume ratio and geometric confinement of electrons. One particularly important property is the localized surface plasmon resonance (LSPR),^[14] which occurs when the oscillation of surface electrons matches the frequency of incident photons. The spectral position and intensity of the LSPR depends not only on the size, shape, composition, and dielectric environment of the metallic nanoparticles (NPs)^[15,16] but also on their aggregation state or assembly.^[17] When metallic NPs are arranged in a chiral geometry,^[18] the coupling of individual plasmons leads to collective plasmon oscillation across the entire structure.^[19] Chiral NP assemblies may exhibit enhanced optical chirality in

Dr. S. Mokashi-Punekar, Y. Zhou, S. C. Brooks, Prof. N. L. Rosi
Department of Chemistry
University of Pittsburgh
Pittsburgh, PA 15260, USA
E-mail: nrosi@pitt.edu

Prof. N. L. Rosi
Department of Chemical and Petroleum Engineering
University of Pittsburgh
Pittsburgh, PA 15260, USA

 The ORCID identification number(s) for the author(s) of this article can be found under <https://doi.org/10.1002/adma.201905975>.

DOI: 10.1002/adma.201905975

the visible region at the frequency of the LSPR, which can be detected using CD spectroscopy (**Figure 2**).^[18,19] The *g*-factor (anisotropy factor), used routinely to compare the optical activity of various chiral systems, is a figure of merit applied to assess the chiroptical response of chiral NP assemblies,^[20–22] and it is defined as the ratio of the molar circular dichroism to the molar extinction.

2. Helical Nanoparticle Assemblies

Because of their unique properties and range of potential applications, chiral NP assemblies have become attractive synthetic targets. Herein, we highlight helical NP assemblies, in particular, as they are known to exhibit exceptionally strong chiroptical activity.^[23] Before delving into the details of specific assembly methods and documenting various examples of helical assemblies, we first set the stage by highlighting some of the milestone achievements in the development of helical NP assemblies and their properties.

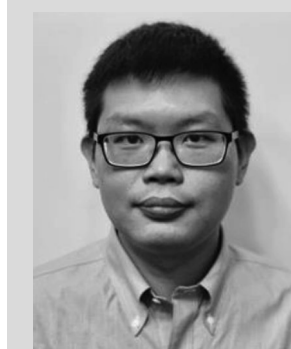
In the late 1990s, which can be considered the “early days” of NP assembly, various biological or bio-inspired templates were used as supports for organizing or growing NPs. More often than not, the resulting NP assemblies adopted the overall shape and dimensions of the template species, yet precision of organization at the individual NP level was lacking. Professor Stephen Mann was an early pioneer in this area, and in 1996 his group reported one of the earliest examples of a chiral NP assembly.^[24] They demonstrated that Au NPs could be deposited onto biolipid tubules in a roughly helical arrangement, following the edges of the helical lipid ribbon. Looking back, this was quite a remarkable achievement, indicating for the first time that patterns on template structures could be transcribed into a chiral NP arrangement. Later, in 2002, Stupp and co-workers used chiral organic templates to grow left- and right-handed cadmium sulfide (CdS) helices,^[25] and shortly thereafter Fu et al. described the synthesis of double-helical Au NP arrays using peptide fibril templates.^[26] These early examples provided precedent and illustrated that chiral nanostructures could be fabricated using template species.

Significant escalation in research activity related to the synthesis and preparation of chiral NP assemblies occurred in the late 2000s, which coincided with the emergence of tunable assembly methods for creating high fidelity superstructures. In 2008, the Rosi group established a synthetic platform for constructing chiral NP assemblies based on rationally designed and highly modular peptide conjugate molecules. As an initial proof of principle, they used their method to construct well-defined double-helical Au NP superstructures.^[27] Some of the first nucleic acid directed chiral NP assemblies were reported shortly thereafter, in 2009. Yan and co-workers used DNA tubules to form left-handed helices of Au NPs,^[28] while Alivisatos and Kotov independently used nucleic acids to link Au NPs into discrete chiral arrangements such as trimers, tetramers, and tetrahedra.^[29,30] Kotov demonstrated that such materials could yield an observable plasmonic CD signal.^[31] Theoretical investigations describing the plasmonic chiroptical properties of these assemblies proceeded in parallel with



Soumitra Mokashi-Punekar

completed his Ph.D. as a research fellow under the mentorship of Prof. Nathaniel Rosi at the University of Pittsburgh. He received a master's degree in chemistry from the Indian Institute of Technology-Bombay in 2014. His research interests include peptide assembly, chiral plasmonic NP assembly, and biomolecule-based hybrid materials.



Yicheng Zhou

received his B.S. degree (2013) from the University of Science and Technology of China. He is now a graduate student at the Department of Chemistry at the University of Pittsburgh. He joined Professor Rosi's group in 2014. His research is in the fields of stimuli-responsive peptide-directed Au NP superstructures.



Sydney C. Brooks

received her B.S. degree in chemistry from West Virginia University, and, in the summer of 2018, joined Prof. Nathaniel Rosi's lab at the University of Pittsburgh for her graduate work. She is currently studying how amino acid modifications affect the structure and assembly of peptide-based NP superstructures.

experimental studies and served as a basis for interpreting physical data and predicting and designing new structures with optimized properties.^[23] Govorov and co-workers have been the forerunners in the theoretical domain, and they predicted that the strongest plasmonic chiroptical signals would be observed for helical NP assemblies.^[32] Their studies establish that the factors influencing chiroptical readout are: i) helix pitch and radius, ii) number of particles per helical turn, and iii) particle size and shape. Synthetic efforts to construct helical NP assemblies intensified significantly following these early demonstrations and theoretical studies. A timeline documenting some of the key advances in the development of helical assemblies is shown in **Figure 3**. In subsequent sections, we detail different assembly methods used for their preparation, citing important examples that illustrate the utility of these methods.

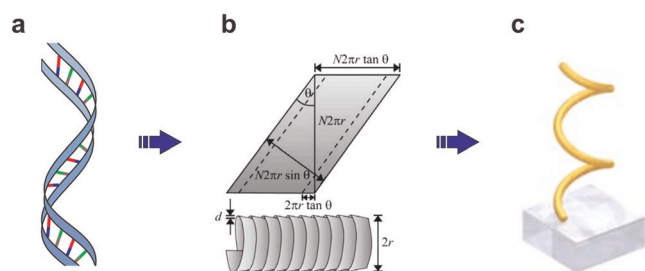


Figure 1. Comparisons and connections between biomolecular chirality and nanomaterial chirality. a) Cartoon representation of a chiral double-stranded DNA molecule that exhibits helical morphology. b) Conceptual design of an artificial chiral helical metamaterial as envisioned by John Pendry in 2004. b) Adapted with permission.^[2] Copyright 2004, American Association for the Advancement of Science (AAAS). c) A schematic representation of a chiral gold helix, constructed using top-down lithographic methods. Adapted with permission.^[3] Copyright 2009, AAAS.

3. Helical Nanoparticle Superstructures: Methods of Construction

3.1. Peptide- and Protein-Directed Nanoparticle Assembly

Peptides are chiral biomolecules and are known to assemble into various fibrillar structures that adopt chiral morphologies including twisted ribbons and helical coils. They are therefore attractive agents for directing the assembly of chiral NP superstructures. Peptide fibrilization was first harnessed for the organization of NPs by Fu et al. in 2003 (Figure 4a).^[26] They prepared helical NP assemblies by combining pre-synthesized colloidal NPs with peptide fibrils, capitalizing on electrostatic interactions between negatively charged NPs and a positively charged peptide to assemble NPs onto peptide fibers. At higher pH, double-helical NP assemblies were the major product for both gold and platinum NPs. Amyloid fibers of bovine insulin have also been used as scaffolds for the deposition of silver NPs (Figure 4b).^[41] We emphasize that there exists a multitude of natural and non-natural peptide- and protein-based chiral fibers, and the two examples detailed above are proof of principle that such fibers can serve as templates for the deposition of inorganic NPs. However, such methods do not allow for a

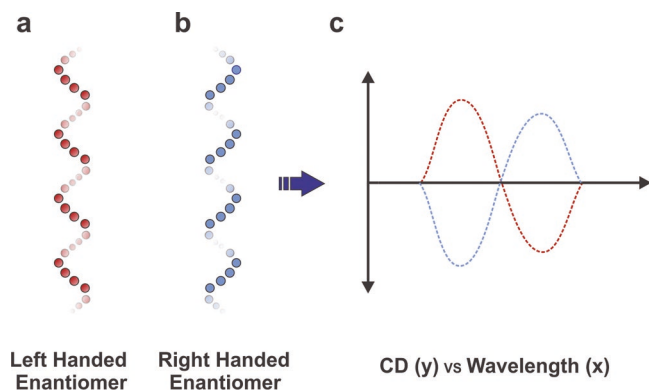


Figure 2. Chiral plasmonic NP assemblies interact differently with circularly polarized light. a) Cartoon representation of a left-handed helical NP assembly. b) Cartoon representation of a right-handed helical NP assembly. c) Left- and right-handed helices produced mirrored CD spectra signals.

sufficient level of synthetic control necessary for fine-tuning structures and optimizing properties.

Rosi and co-workers developed a peptide-based synthetic platform for designing and preparing a diverse collection of helical Au NP assemblies and systematically tuning their architectures and properties.^[22,27,42–44] Their synthetic methods rely on highly tailorable peptide conjugate molecules that not only play an integral role in regulating NP synthesis and growth by adhering to Au NP surfaces but also direct NP assembly. The peptide conjugates, R-PEP_{Au}, consist of an Au binding peptide^[45] (PEP_{Au}, AYSSGAPPMPF) tethered to an “R” group, which is typically an aliphatic carbon chain. The peptide sequence and the “R” group can be independently adjusted to affect the structure and morphology of the helical assembly. From a practical perspective, the methodology combines NP synthesis and assembly into a single step; that is, as the particles nucleate and grow, they also assemble together into the product superstructure. This stands in contrast to most other methods of helical NP assembly (vide infra), which require multiple preparative steps including NP synthesis, NP functionalization and purification, template synthesis and purification, and finally superstructure assembly.

In 2008, as a first example of this assembly strategy, C₁₂-PEP_{Au} peptide conjugate molecules were used to prepare Au NP double helices (Figure 4c).^[27] Consisting of fairly monodisperse NPs (≈8 nm) and having a periodic pitch of ≈83 nm, these assemblies were one of the first well-defined chiral NP superstructures and clearly demonstrated the unique utility of the methodology. The structural fidelity of the assemblies underlined their potential for exhibiting well-defined plasmonic chiroptical properties. Importantly, a molecular model for the peptide fiber was developed that served as a foundation for future hypothesis-driven assembly studies aimed at logically tuning structure and properties. Building on this model, the Rosi group showed that the handedness of the superstructure was controlled by the chirality of the constituent amino acids (Figure 4d).^[36] L-Amino acids yielded left-handed double helices and D-amino acids yielded right-handed double helices, and they exhibited mirror-image CD signatures, as predicted by theory. This was the first demonstration that peptide molecular structure could be adjusted to control the assembly and properties of helical superstructures. Thus, with the development of this family of Au NP double helices, a robust and tunable molecular platform for constructing helical NP assemblies and adjusting their physical properties was established.

A variety of other helical Au NP superstructures were also prepared using this peptide-based methodology.^[43,44,46] Of particular interest due to their intense chiroptical properties are a class of single-helical Au NP assemblies constructed using C_x-(PEP_{Au}^{M-ox})₂ (x = 16–22, M-ox indicates methionine sulfoxide), which consists of two PEP_{Au} attached to an aliphatic tail (Figure 4e–g).^[22,47] This series of peptide conjugate molecules assemble into helical ribbons whose pitch length increases with increasing aliphatic tail length. As a consequence, these conjugates can be used to prepare a family of Au NP single helices having incrementally variable pitch: ≈80 nm for C₁₆-(PEP_{Au}^{M-ox})₂ and up to ≈125 nm for C₂₂-(PEP_{Au}^{M-ox})₂ (Figure 4f).^[47] Plasmonic chiroptical response is predicted to be inversely proportional to pitch, which is verified by the

Major Highlights in Helical Nanomaterial Synthesis (2002–Present)

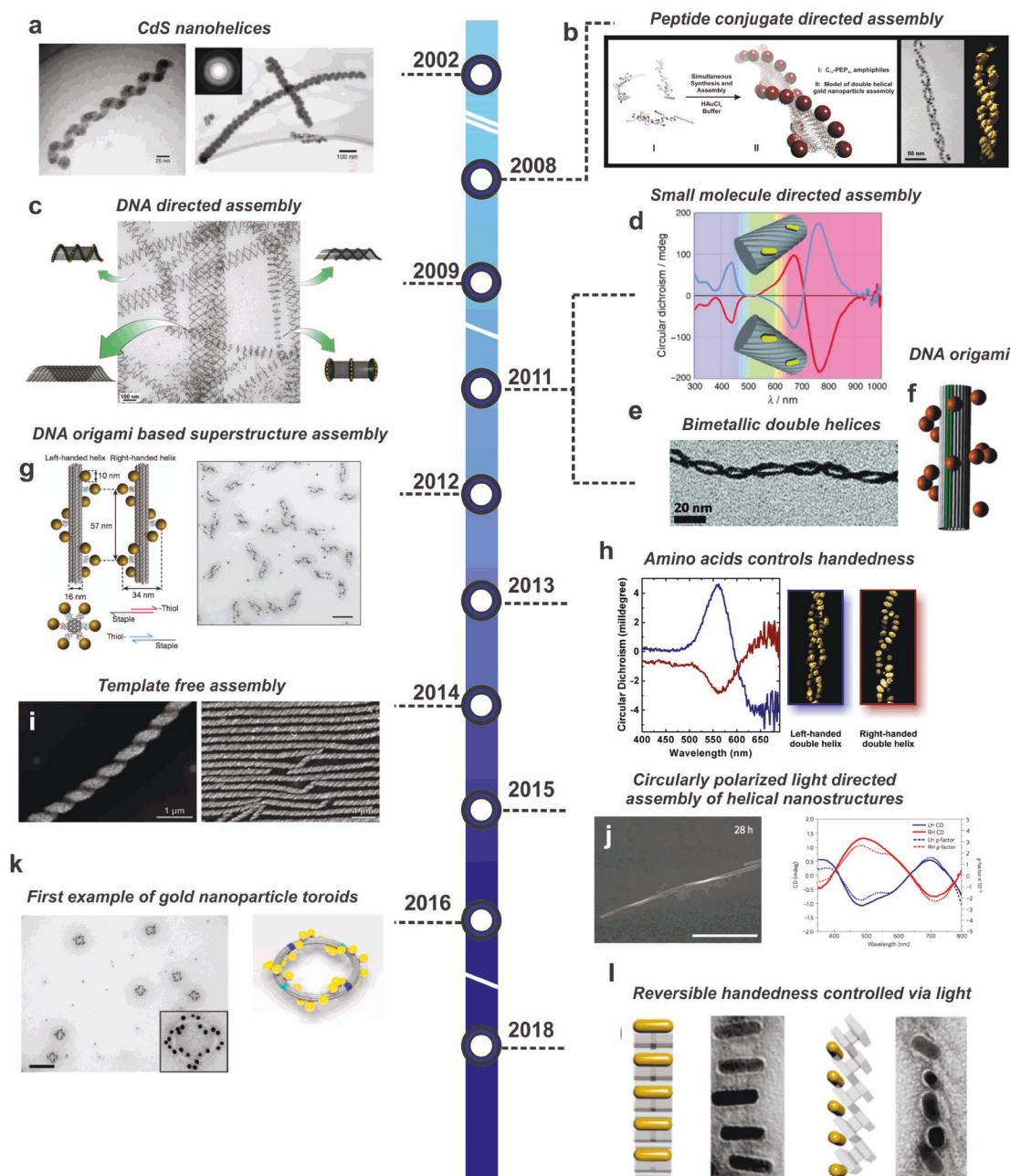


Figure 3. Major highlights in the synthesis of helical nanomaterials since 2002. a) TEM images of helical CdS assemblies. Adapted with permission.^[25] Copyright 2002, Wiley-VCH. b) Schematic illustration, TEM image, and 3D tomographic volume of double-helical Au NP assemblies prepared using rationally designed peptide conjugate molecules. Adapted with permission.^[27] Copyright 2008, American Chemical Society. c) Helical Au NP superstructures prepared using DNA tubules. Adapted with permission.^[28] Copyright 2009, AAAS. d) Au nanorods assembled on oxalimide-based fibers. These structures were some of the first to exhibit strong plasmonic chiroptical activity. Adapted with permission.^[21] Copyright 2011, Wiley-VCH. e) TEM images of bimetallic nanowire double helices consisting of an Au–Ag alloy. Adapted with permission.^[33] Copyright 2011, American Chemical Society. f) One of the earliest examples of Au NP single helices constructed using DNA origami assembly methods. Adapted with permission.^[34] Copyright 2012, American Chemical Society. g) High-fidelity Au NP single helices prepared using DNA origami, which exhibited exceptional chiroptical properties. Adapted with permission.^[35] Copyright 2012, Springer Nature. h) Handedness and plasmonic chiroptical properties of Au NP double helices constructed using peptide conjugate molecules could be controlled via the chirality of the constituent amino acids. Adapted with permission.^[36] Copyright 2013, American Chemical Society. i) Template-free assembly of magnetite nanocrystals into helical superstructures. Adapted with permission.^[37] Copyright 2014, AAAS. j) Circularly polarized light was used to influence the chiral assembly of CdTe NPs into nanohelices with specific handedness. Adapted with permission.^[38] Copyright 2015, Springer Nature. k) Unique left- and right-handed toroidal Au NP metamaterials assembled using DNA origami templates. Adapted with permission.^[39] Copyright 2016, American Chemical Society. l) An early example of dynamic Au NP helical assemblies, where the handedness of the helices can be controlled via photoresponsive moieties. Adapted with permission.^[40] Copyright 2018, American Chemical Society.

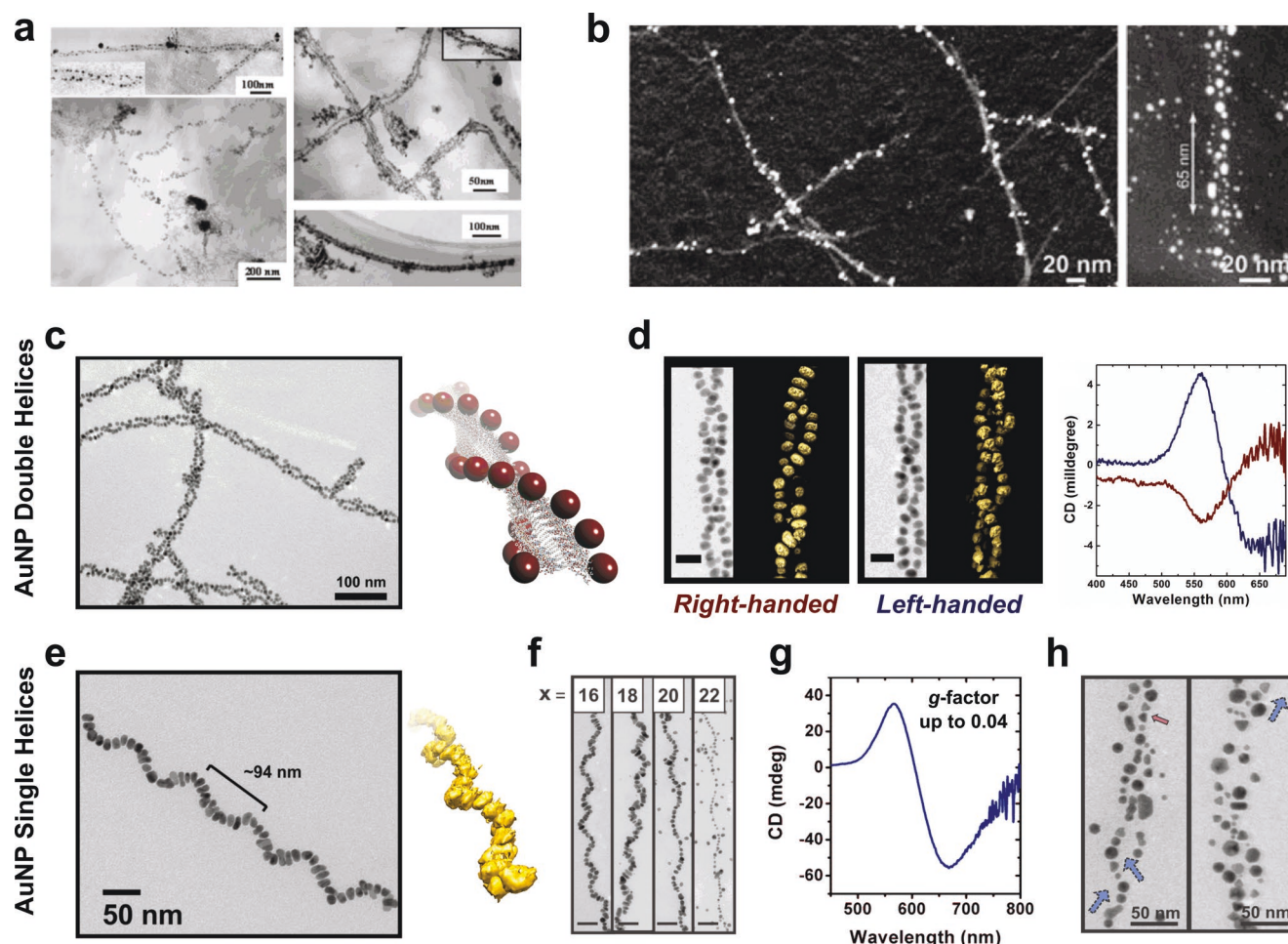


Figure 4. Peptide-based helical NP assemblies. a) One of the first papers using peptides for NP assembly exploited the natural phenomenon of peptide fibrilization. Electrostatic interactions between the positively charged nanofibrils and the negatively charged presynthesized Au and Pd NPs drove the superstructure assembly. Adapted with permission.^[26] Copyright 2003, Wiley-VCH. b) Amyloid fibrils polymerized from bovine insulin served as a scaffold for silver NP assembly. Adapted with permission.^[41] Copyright 2010, Wiley-VCH. c) An amphiphilic peptide conjugate molecule, C_{12} -PEP_{Au}, that assembles into fibers was used to direct the assembly of double-helical Au NP superstructures. Adapted with permission.^[27] Copyright 2008, American Chemical Society. d) Chirality of the constituent amino acids of C_{12} -PEP_{Au} determine superstructure chirality and mirrored chiroptical signals were observed. Adapted with permission.^[36] Copyright 2013, American Chemical Society. e) Single-helical Au NP structures produced from the amphiphilic peptide conjugate C_{18} -(PEP_{Au}^{M-ox})₂. Adapted with permission.^[22] Copyright 2016, American Chemical Society. f) Increasing the aliphatic tail length of C_x -(PEP_{Au}^{M-ox})₂ gave rise to a longer helical pitch. Adapted with permission.^[47] Copyright 2017, American Chemical Society. g) Strong plasmonic chiroptical response was observed for helices constructed using C_{18} -(PEP_{Au}^{M-ox})₂. Adapted with permission.^[22] Copyright 2016, American Chemical Society. h) Adding auxiliary particle capping reagents can lead to anisotropic particle growth, resulting in helices containing a large number of anisotropic Au NP. Adapted with permission.^[48] Copyright 2018, Wiley-VCH.

experimentally observed CD signal intensities for this collection of helices. The single helices prepared using C_{16} -(PEP_{Au}^{M-ox})₂ and C_{18} -(PEP_{Au}^{M-ox})₂ exhibit significant plasmonic chiroptical response, with optimized *g*-factors of ≈ 0.02 – 0.04 that rank among the highest reported for helical NP assemblies (Figure 4g).

Because these methods combine NP synthesis and assembly into a single preparative step, other reagents can be added to the syntheses to affect NP growth and synthetic conditions can be modified to affect superstructure metrics and morphology. For example, when auxiliary particle capping agents such as citrate are added to the double helix synthesis, the product helices consist of smaller gold particles (≈ 6 nm on average; cf. ≈ 8 nm for double helices described above).^[36,42] Rosi and co-workers

recently demonstrated that the shape of Au NPs within the single-helical superstructures could be modulated through the addition of external surfactants such as cetyltrimethylammonium bromide (Figure 4h).^[48] These surfactants lead to anisotropic growth and the formation of hexagonal and prismatic particles within the helices.

Peptides can also be designed to assemble and coil around nanomaterial templates and present nucleation sites for the growth of inorganic NPs. Kang et al. designed a composite material consisting of a carbon nanotube (CNT) surrounded by an engineered peptide.^[49] The peptide sequence was designed to assemble into helices, where one face had an affinity for the CNTs and the other would bind the inorganic NPs. A 30-residue peptide sequence, HexCoil-Ala, was used, which forms

an antiparallel hexameric bundle via helix–helix interactions. The resulting superhelix coils along the axis of the CNT. HexCoil-Ala was genetically modified to include cysteine residues on the outer face of the coil for particle binding. Computational studies were used to direct the modifications to the peptide sequence in order to obtain the desired geometry. The addition of gold and platinum ion sources produced well-alloyed NPs at the designated locations along the peptide coil, forming a triple-helical NP assembly. This bimetallic system has great potential in electrocatalytic applications, specifically oxygen reduction, as demonstrated by the authors.

The representative examples detailed above clearly show the potential of peptides and peptide-based molecules as highly tunable and versatile assembly agents for the construction of helical NP superstructures. To date, however, most peptide-based helical NP superstructures are static, despite the fact that peptides and peptide assemblies are often dynamic and can be designed to respond to external stimuli. The design and synthesis of dynamic and responsive peptide-based NP assemblies is certainly an area of opportunity and is expected to be “fertile ground” in the next phase of development for this class of materials. Further, there are also opportunities to explore in more depth how peptide sequence affects NP growth, assembly, and the metrics of helical NP superstructures. With 20 natural and hundreds of non-natural amino acids to choose from, variation to known sequences and new sequence motifs may lead to heretofore unobserved helical chiral architectures. The vast sequence space will necessitate engagement with computational colleagues to develop predictive models that help guide peptide sequence design.

3.2. DNA-Directed Nanoparticle Assembly

Some of the most structurally intricate nanomaterials have been constructed with nucleic acid building blocks due to their sequence-specific base-pairing and exceptional programmability.^[50,51] DNA tiles can be linked together to form different geometrical entities, and DNA origami methodology can be used to create unusual structures with high fidelity. DNA-based nanostructures can be designed to associate with oligonucleotide-functionalized NPs to create NP superstructures.

To our knowledge, Yan et al., in 2009, presented the first example of nucleic acid-directed assembly of helical NP superstructures (Figure 5a).^[28] In this report, they co-assemble DNA and oligonucleotide functionalized Au NP precursors into 3D tubules that present the NPs into helical arrays and other architectures, including stacked rings. This first example of using DNA to construct helical NP assemblies showcased the versatility of DNA as a building block for NP superstructures and opened the proverbial floodgates to exploration in this area.

DNA origami approaches have attracted significant attention and have proven very versatile for creating a wide array of helical superstructures due to the precise level of control over the size and shape of the origami template and the number and location of NP binding sites on the template. In 2011, Liu and Ding's group designed a 2D DNA origami template that could be rolled-up into a 3D tube with helically arranged NP binding sites (Figure 5b).^[34] They decorated a 2D DNA origami sheet

with two parallel NP binding sites onto which oligonucleotide functionalized Au NPs could hybridize. The sheets were “rolled” into hollow tubes through the addition of folding strands that linked opposite sheet edges; a direct consequence of the rolling was the alignment of the NPs into a helical arrangement, which resulted in a chiroptical response at the frequency of the LSPR. A contemporaneous report from Liedl and co-workers, which uses a similar assembly approach, set a new standard for high fidelity DNA-based helical superstructures (Figure 5c).^[35] Using 24-helix bundles with nine helically arranged hybridization sites for oligonucleotide-modified Au NPs, they prepared left- and right-handed Au NP helices with exceptionally high yield (96% and 98% site attachment and 77% and 86% perfect assembly for left- and right-handed helices, respectively). Significantly, the helices displayed strong plasmonic chiroptical activity which could be dramatically enhanced via secondary deposition of additional gold or silver, leading to demonstration of their application as a “metafluid.” These benchmark results redefined the landscape of the chiral nanostructure field, further inspiring new studies and highlighting the potential of helical NP superstructures for real applications.

The groundbreaking work by Liu, Ding, and Liedl unleashed a flurry of new DNA origami-based assembly methods for constructing helical NP superstructures. Shen et al. encased a gold nanorod (Au NR) in DNA origami to create a hybrid core onto which spherical Au NPs were arranged in a helical fashion (Figure 5d).^[52] This original approach provided a route toward the formation of hetero-NP assemblies comprising more than one kind of NP. Helical assemblies can also consist entirely of Au NRs: a ladder of periodically offset Au NRs will exhibit a helical, twisted ribbon morphology. To access such structures, Wang and co-workers designed an “X” pattern of capture strands on two opposite surfaces of square DNA origami sheets (Figure 5e).^[53] Combining these sheets with DNA-decorated Au NRs resulted in a twisted ribbon of Au NRs, with adjacent rods axially offset by 45°. The handedness of the Au NR twisted ribbons could easily be tailored by using a mirror image of the “X” pattern. Adjusting the ratio of origami:Au NR allowed for increasing the average number of Au NR per ribbon, which led to an increase in the intensity of the plasmonic CD signal. Origami approaches have also been employed to fabricate toroidal superstructures, which is essentially a closed loop helix. Liu's group stitched together four curved DNA origami monomers in a head-to-tail fashion to create a closed loop (Figure 5f).^[39] If anchoring strands are appropriately positioned along the loop, oligonucleotide-functionalized Au NPs will adopt a toroidal arrangement.

In all the preceding examples, complementary base pairing leads to the structure of the underlying DNA-based template. Cecconello and co-workers devised an alternative approach that relies on “promoter strands” to induce curving of a DNA-based sheet (Figure 5g).^[54] The sheet was decorated with both tether strands for anchoring Au NP as well as “promoter strands.” Steric and electrostatic repulsions between the “promoter strands” force the sheet to curve into a barrel-like structure that presents the tether strands in a helical array. Both left- and right-handed helical NP superstructures, which both display plasmonic chiroptical activity, were constructed.

Like the peptide-based helical NP superstructures, most of the reported DNA-based structures are static. An emerging area

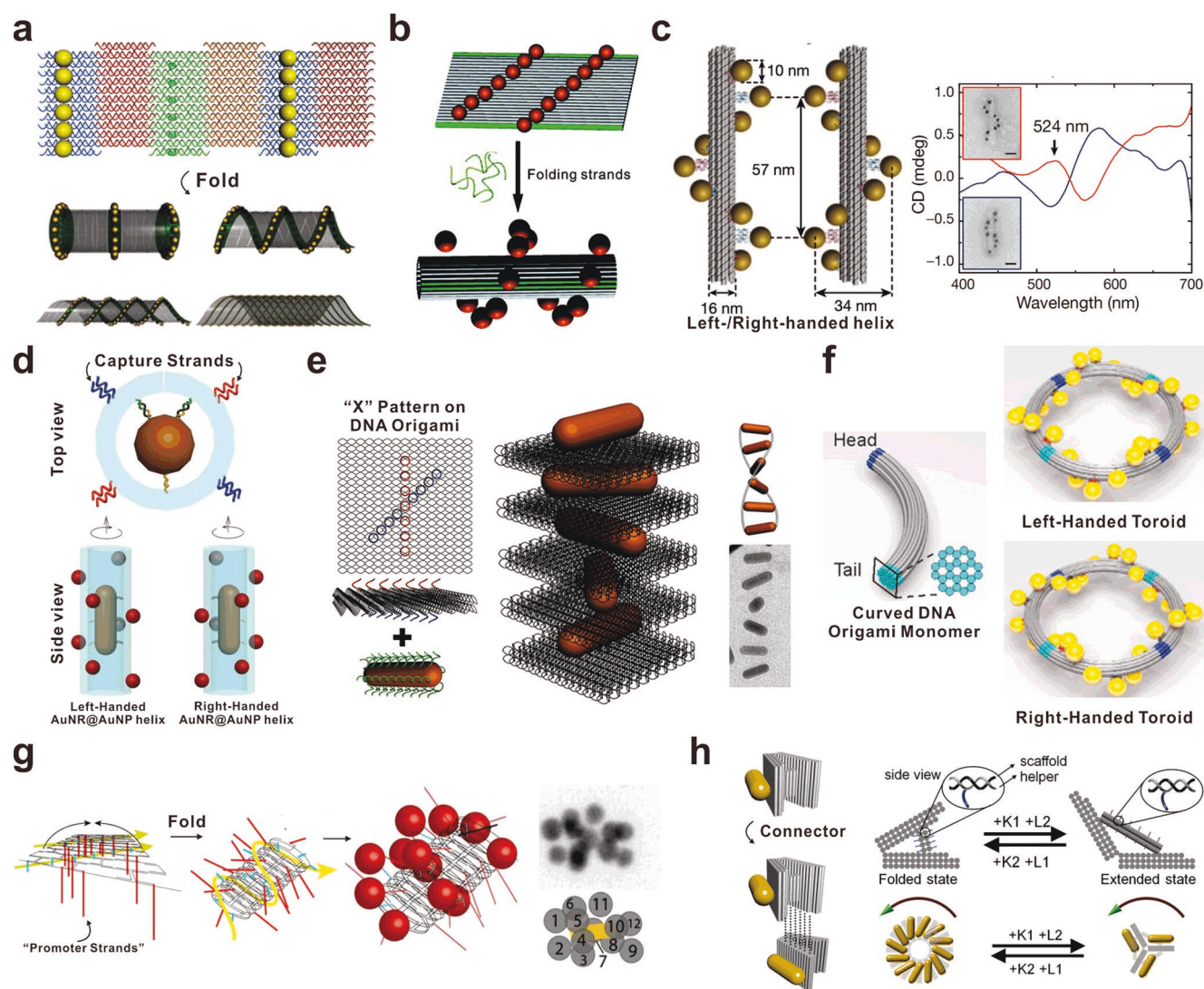


Figure 5. Helical DNA-based NP superstructures. a) Multiple Au NP assemblies including stacked rings, single spirals, double spirals, and nested tubules were formed by rolling-up an Au NP decorated DNA tile. Adapted with permission.^[28] Copyright 2009, AAAS. b) Parallel lines of Au NPs were anchored onto a DNA tile, which was then joined together by addition of folding strands, thus forming a helical Au NP assembly directed by DNA. Adapted with permission.^[34] Copyright 2012, American Chemical Society. c) Right- and left-handed Au NP helices with high yield were formed by anchoring Au NPs onto a DNA origami core template in a helical fashion. Left-handed (red) and right-handed (blue) signals were also observed in the CD spectra. Adapted with permission.^[35] Copyright 2012, Springer Nature. d) Left- and right-handed Au NP helices were assembled by decorating a DNA origami wrapped Au NR. Adapted with permission.^[52] Copyright 2017, Wiley-VCH. e) DNA origami sheets were used to form helical arrangements of Au NRs. Adapted with permission.^[53] Copyright 2015, American Chemical Society. f) Four curved DNA origami rods were joined together, forming a toroidal scaffold for Au NPs. Adapted with permission.^[39] Copyright 2016, American Chemical Society. g) Helical superstructures were constructed using a DNA origami barrel. Adapted with permission.^[54] Copyright 2016, American Chemical Society. h) Dynamic assembly of twisted Au NR helices was formed by a V-shaped DNA origami. Adapted with permission.^[40] Copyright 2018, American Chemical Society.

is the fabrication of dynamic superstructures. Lan, Govorov, and Liu recently reported a strategy for dynamically tuning the superstructure helicity (Figure 5h).^[40] Using designed DNA “switches” that could affect structure of the DNA template, they were able to create helical Au NR superstructures that underwent shifts between left- and right-handedness as well as folded and extended states. These transformations, respectively, manifest as either an inversion of the plasmonic chiroptical response (left- to right-handed) or a significant dampening of the signal (folded to extended). Looking into the future, research into DNA-based dynamic helical assemblies will likely intensify,

with a particular focus on exploration of new switching modalities with rapid response times.

3.3. Other Assembly Methods

3.3.1. Organic-Molecule-Directed Nanoparticle Assembly

One of the earliest examples of helical NP assemblies prepared using an organic scaffold was reported by the Stupp lab. Sone et al. used previously reported “dendron rodcoils” (DRC)

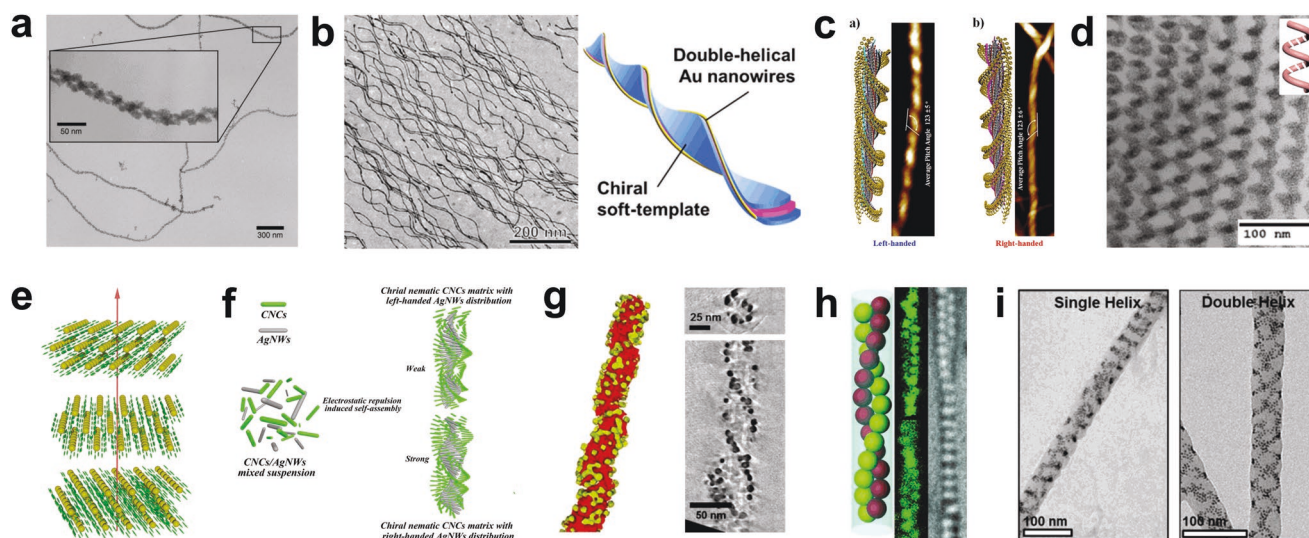


Figure 6. Templated assembly of helical NP superstructures. a) CdS helices templated on triblock dendron rodcoil (DRC) nanoribbons. Adapted with permission.^[55] Copyright 2005, Wiley-VCH. b) Nanowires grown on a template composed of a bicomponent organogelator, with one component directing the chirality of the structures and the second acting as a capping agent for NP growth. Adapted with permission.^[57] Copyright 2018, American Chemical Society. c) A modular gelator system was used to assemble Au NPs into left- and right-handed helices. Adapted with permission.^[61] Copyright 2014, American Chemical Society. d) A block copolymer was synthesized with helical pores with controlled chirality for NP assembly. Adapted with permission.^[62] Copyright 2017, American Chemical Society. e) Au NPs coated with a chiral liquid crystal ligand assemble into layers which then stack into chiral 3D arrangements. Adapted with permission.^[64] Copyright 2015, American Chemical Society. f) The electrostatic interactions between cellulose nanocrystals and Ag NWs were exploited to produce helical assemblies with chirality control. Adapted with permission.^[65] Copyright 2015, American Chemical Society. g) Functionalized helical silica templates were decorated with Au NPs. Adapted with permission.^[69] Copyright 2017, American Chemical Society. h) Silica and polystyrene colloidal spheres were assembled within sodium dodecyl sulfate and β -cyclodextrin microtubules, with double-helical arrangements produced at optimal sphere and microtube diameters. Adapted with permission.^[70] Copyright 2013, Wiley-VCH. i) With an anodic aluminum oxide membrane serving as cylindrical confinement, a block copolymer and presynthesized Au NPs formed a variety of superstructures, including single and double helices. Adapted with permission.^[71] Copyright 2017, American Chemical Society.

as a template for generating CdS nanocoils, which have potential applications in photovoltaics due to the semiconducting nature of the material.^[25] The triblock DRC molecules assemble into nanoribbons via hydrogen bonding, and in certain solvents, these ribbons twist into both left- and right-handed helices. CdS mineralization predominantly yielded single helices with a pitch length of approximately twice that of the original ribbons. When CdS was mineralized with aged DRC samples, double helices were the dominant product (**Figure 6a**).^[55] In order for double helices to form, the authors assume that both faces of the ribbon must be equivalent, and any inequality between the two faces would cause one to be more susceptible to CdS mineralization, therefore yielding single helices. CdS NPs have also been assembled on lipid membranes. Specifically, Zhou et al. formed helical assemblies of CdS on a lipid nanotube template composed of a glycolipid, *N*-(11-*cis*-octadecenoyl)- β -D-glucopyranosylamine functionalized with the chiral additive aminophenyl- β -D-glucopyranoside.^[56]

Organic scaffolds have also been used to assemble noble metal nanomaterials. Nakagawa and Kawai developed a method to synthesize helical gold nanowires (Au NWs) utilizing a bi-component soft chiral template (**Figure 6b**).^[57] The first component, chiral D-12-hydroxystearic acid (D-HSA) and its enantiomer L-HSA, directed the chirality of the structures, and the second component, a long chain amidoamine (C₁₈AA), served as a capping agent for controlling the nanocrystal growth. When the two components were mixed together, they formed a stable hydrogel with a twisted ribbon morphology. The Au NWs grew

along the edges of the ribbons, yielding a double-helical structure with handedness corresponding to the organogelator template. The left- and right-handed structures exhibited mirrored CD signals in the 400–800 nm range of the visible spectrum.

George et al. utilized a thermally responsive organic template in order to synthesize chiral Au NP assemblies that remained stable after the removal of the underlying scaffold.^[58] The template consisted of a molecule with a hydrophobic core flanked by two Boc-protected D- or L-alanines, which assembled into chiral nanofibers. These nanofibers were then functionalized with Au NP seeds, and after the addition of a gold ion source, chiral NP assemblies were grown on the nanofibers. The assemblies contained between 5–7 NPs, which amounted to a full turn of the helical arrangement, and presumably prevented any further growth from occurring. A strong, mirrored plasmonic signal was observed for the structures. Additionally, when the temperature was raised, the organic template decomposed, leaving behind the stable NP assemblies.

3.3.2. Polymer-Mediated Nanoparticle Assembly

The first major report documenting the use of polymeric materials to direct the formation of helical NP assemblies was published in 2005.^[59] A double hydrophilic block copolymer (DHBC) directed the assembly of BaCO₃ nanocrystals into a chiral helical structure. One block with a strong affinity for BaCO₃ was designed to bind the NPs while the other

hydrophilic block promoted assembly. The resulting helical structures were produced in extremely high yield ($\approx 90\%$). Oh et al., in 2010, designed a polymeric scaffold to assemble Au NP helices that showed a plasmonic response.^[60] Specifically, they doped a chiral poly(fluorene-*alt*-benzothiadiazole) (PFBT) with Au NPs to form nanocomposite films. In this system, differential chiroptical activity was observed depending on the annealing of nanocomposite films. A second example published by Jung et al. also used chiral building blocks to produce helical Au NP superstructures (Figure 6c).^[61] Two different chiral compounds were used to induce left- and right-handed helicity into the assemblies of a molecular gelator. Au NPs were grown onto the chiral molecular assemblies to yield helical NP superstructures whose optical properties could be tuned by synthetically adjusting the size of the component NPs.

Block copolymers (BCP) like the first example discussed in this section are often employed to organize NPs into well-defined architectures. These molecules exhibit programmable self-assembly due to their chemically unique segments. Lu et al. used a cross-linked BCP films containing helical pores as templates for organizing Au NPs into helical architectures (Figure 6d).^[62] The handedness of the pores was controlled via the addition of either D- or L-tartaric acid, and the Au NP superstructures displayed an optical response correlating with the handedness of the film.

3.3.3. Nanoparticle Assembly via Liquid Crystals

Liquid crystalline materials can form highly ordered long range assemblies, guided by intermolecular interactions or external stimuli. In 2004, Mitov et al. used the periodicity of liquid crystals to induce long-range ordering of NPs.^[63] A cholesteric liquid crystal with a helical structure was doped with platinum NPs. The NPs showed an affinity for regions where the liquid crystal molecules were parallel to the film plane and thus arranged into ribbons that mimicked the fingerprint pattern of the liquid crystal. The distance between NP ribbons depended on the chirality of the cholesteric carrier and could be controlled by adjusting the helical pitch. Cholesterol liquid crystals were also used by Cseh et al. (Figure 6e). They functionalized Au NPs with a chiral liquid crystal ligand which directed a chiral arrangement of the NPs.^[64] The helicity of these structures originates from offset stacking of layers of NP chains, and a small offset angle between neighboring layers results in mesoscopic winding of NP layers around a central axis.

Similar to cholesteric liquid crystals, cellulose liquid crystals are commonly used NP assembly agents, because they show good dispersibility in water and arrange in a parallel, lyotropic fashion. Chu et al. published a detailed systematic study describing the assembly of silver nanowires (Ag NW) via cellulose nanocrystals (CNCs).^[65] The assembly was controlled by the electrostatic interactions between the CNCs and Ag NW, two negatively charged species, as shown in Figure 6f. The CNCs also have electrostatic repulsions with neighboring nanocrystals. As these repulsive interactions increase, the Ag NWs transition from spontaneously formed left-handed helices to right-handed helices, as a way of minimizing the systems' free energy. Majoinen et al. also used CNCs for NP assembly,

taking advantage of the right-handed chirality of the individual crystals.^[66] In this case, electrostatic attraction between negatively charged CNCs and positively charged Au NPs drove the assembly. By optimizing the size of the Au NPs relative to the CNCs, a strong plasmonic chiroptical signal was produced, indicative of a right-handed helix.

Wang et al. observed interesting chiroptical properties in a system resembling a liquid crystalline material which was composed of Au NRs assembled on a scaffold of surfactant molecules and phospholipid film.^[67] Presynthesized Au NRs stabilized with cetyltrimethylammonium bromide (CTAB) were added to a dried thin film of 1,2-dimyristoyl-sn-glycero-3-phosphatidylcholine (DMPC) and a fluorescence labeled lipid, rhodamine B 1,2-dihexadecanoyl-sn-glycero-3-phosphoethanolamine, triethylammonium salt (Rhodamine DHPE). After rehydration and an incubation period, the system showed a plasmonic response due to the arrangement of the Au NRs when investigated via CD spectroscopy. This chiroptical response served as evidence to the formation of an ordered helical arrangement of the Au NRs on the chiral hybrid superstructure.

3.3.4. Silica-Based Inorganic Scaffolds

Silica-based inorganic scaffold materials can also be utilized for the assembly of helical NP superstructures, as demonstrated by Oda and co-workers.^[68] They used sol-gel transcription of surfactants in the presence of a chiral counterion to prepare silica helices with tunable structural parameters. After functionalizing the helices with either thiol or amine groups, pre-synthesized Au NPs were adsorbed onto their surface to form helical NP superstructures. In a later report published in 2017, various reducing and stabilizing methods were screened for functionalizing the silica scaffolds with Au NPs (Figure 6g).^[69] The authors determined that the plasmonic chiroptical response of these materials was dependent on the size of the Au NPs as well as the homogeneity of the Au NP arrangement.

3.3.5. Nanoparticle Assembly via Space Confinement

Helical arrangements can also be produced by confining NPs within a template. In one example, Jiang et al. used a sodium dodecyl sulfate (SDS) and β -cyclodextrin (β -CD) microtube to confine colloidal silica and polystyrene spheres into helical chain structures within the microtube pores (Figure 6h).^[70] The assembly was reversible via thermal control, and the approach was applicable to a variety of colloids. Control over the tube diameter also led to other structural morphologies besides the helical arrangement. In an example using metallic NPs, Bai and co-workers designed a supramolecular scaffold consisting of a block copolymer, polystyrene(19 kDa)-*block*-poly(4-vinylpyridine) (PS-*b*-P4VP), with a small molecule, 3-*n*-pentadecylphenol (PDP), hydrogen bonded to the 4VP unit (Figure 6i).^[71] This supramolecular construct and Au NPs were drop cast into an anodic aluminum oxide (AAO) membrane, which provided cylindrical confinement for the composite mixture. Confinement effects coupled with favorable interactions between the NPs and the supramolecular unit resulted in formation of a

variety of superstructure morphologies including single and double helices.

3.3.6. Template-Free Assembly Methods

The helical NP superstructures discussed above all require some type of scaffold or molecular entity to direct assembly; however, not all reported structures require an underlying template. Kotov and co-workers have published numerous accounts of helical nanostructures derived from NP precursors. Srivastava et al. demonstrated that flat ribbons of cadmium telluride (CdTe) nanocrystals could be converted to helical structures upon irradiation with visible light (Figure 7a).^[72] Equal amounts of left- and right-handed helices were formed, and the driving force was determined to be electrostatic interactions between the component nanocrystals. In a subsequent study, the Kotov group used CdTe twisted ribbons prepared with thioglycolic acid as a stabilizer as templates for Au NP assembly.^[73] In further development of this unique system, they demonstrated that irradiation of CdTe nanocrystals with either right- or left-circularly polarized light induced formation of an excess of either right- or left-handed twisted ribbons, respectively.

Helical superstructures have also been synthesized via functionalization of discrete NPs with a chiral ligand. In the next example, inorganic superstructures were formed by cysteine-functionalized NPs, where the chiral form of the amino acid determined the handedness of the helices formed. Zhou et al. coated chiral CdTe NPs with cysteine, which then helically assembled around Te nanowire cores.^[74] Because these structures exhibit high enantiomeric purity and display chiroptical activity in the visible region of the spectrum, this work presented a simple yet effective way to translate chirality from the molecular scale to the nanoscale. Cadmium selenide (CdSe) NPs have also been assembled using other small molecule ligands. Jana et al. showed that flat CdSe platelets, originally stacked in a linear arrangement, twist helically after functionalization with oleic acid (Figure 7b).^[75] With the addition of oleic acid to native CdSe structures prior to solvent evaporation, a flat ribbon was formed, but incremental addition of oleic acid throughout the drying process yielded helical product structures. The twisted structure was linked to the inhomogeneity of the ligand conformations, dependent upon the binding location on the nanoplatelet face. These interactions led to a mechanical stress that twisted the CdSe ribbon into a helical structure.

Alloyed plasmonic metals have also been incorporated into helical nanoscale assemblies. In 2011, Wang et al. reported an Au-Ag alloy nanowire that twists into a double helix when a thin metal layer was grown on its surface (Figure 7c).^[33] The twisting was linked to the underlying chirality of the original nanowire. The composite nanowire was determined to have a Boerdijk–Coxeter–Bernal (BCB) lattice, which is composed of lattice units that cannot pack closely. As the diameter of the wire increased with the deposition of the additional metal layer, the lattice strain increased until the nanowire wound around itself, forming the double-helical structure.

External stimuli, such as light irradiation discussed above, can be used to initiate the assembly of inorganic NPs. One interesting example shown in Figure 7d, published by

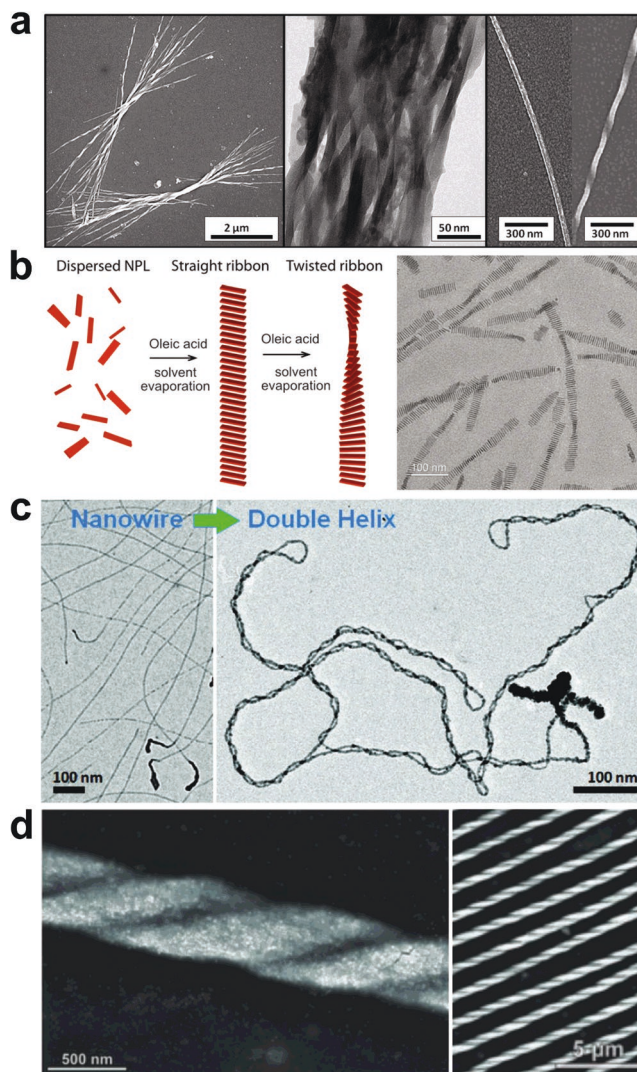


Figure 7. Template-free assembly of helical NP superstructures. a) CdTe/CdS ribbons were twisted into left- and right-handed helices with irradiation of visible light, relieving the mechanical stress caused by CdS photo-oxidation. Adapted with permission.^[72] Copyright 2010, AAAS. b) CdSe nanoplatelets formed a variety of superstructures with different methods of oleic acid functionalization. Adapted with permission.^[75] Copyright 2017, AAAS. c) Au-Ag alloy nanowire that transitions into a double helix with the growth of a thin metal layer. Adapted with permission.^[33] Copyright 2011, American Chemical Society. d) Magnetite cubes were assembled at the liquid–air interface due to the presence of an external magnetic field. Adapted with permission.^[37] Copyright 2014, AAAS.

Singh and co-workers, used an applied magnetic field to assemble magnetite nanocubes (NCs).^[37] The resulting structures depended on the NC density at the liquid–air interface during synthesis and the intensity of the external magnetic field. As the field intensity increased, the dipoles of the NCs aligned parallel, and the resulting repulsion between laterally adjacent NCs caused periodic spacing between the columns of NCs. When the cubes were rotated 45°, the belts twisted at higher magnetic field intensities giving rise to helical structures. Simulations confirmed that the twisted morphology was accompanied by a decrease in free energy. At relatively low

intensities, both left- and right-handed helices were observed, but as the intensity was increased large regions of “enantiopure” helices were observed due to the need for tight packing. Additionally, at higher intensities the belts widened, yielding double and triple stranded helices.

It is clear that, in addition to the peptide- and nucleic acid-based methods described in previous sections, a wide variety of other molecular agents can be used to direct the assembly of helical NP superstructures. In addition, a number of template-free methods have also been developed that use small molecules or even external forces or fields to direct NP assembly. These are particularly attractive areas of inquiry, especially when considering cost and scale: less expensive assembly methods will most likely be necessary to move helical NP superstructures into widespread applications. We note that, unlike most peptide and nucleic acid methodologies which yield enantiopure products, many of the methods discussed in Section 3.3 produced mixtures of both right- and left-handed helices, with some exceptions. An area of opportunity may be to more broadly explore the use of chiral additives that can bias the production of one enantiomer over the other, exploiting the “Sergeants and Soldiers” principle.^[76] Thinking further, one can imagine using chiral additives to reversibly switch handedness of a given helical system.

4. Applications and Outlook

The assembly of helical NP superstructures has advanced significantly over the last 10 years, and new methods of assembly and strategies for controlling helix geometry and metrics are surely forthcoming. To date, applications of these materials are more often proposed rather than demonstrated. It is expected that, in the coming years, more effort will be dedicated to examining optoelectronic, sensing, and catalysis applications. Liz-Marzán and co-workers recently provided a beautiful example of how helical nanoscale chirality can be harnessed for the detection of protein aggregation, specifically amyloid fibrils, which are linked to many neurodegenerative diseases.^[11] They demonstrated that Au NRs assembled onto amyloid fibers to generate a chiral double-helical arrangement that displayed an enhanced plasmonic chiroptical signal, indicating the presence of the amyloid. This method was expanded to detect infectious recombinant prions as well as α -synuclein fibrils, hinting at a wide variety of possible disease-related targets.

As this field continues to progress toward applications, it will become important to consider cost and scale of the syntheses. This report clearly indicates that many of the reported examples are based on either peptides or nucleic acids. The use of these molecules does not necessarily preclude scalable and economical syntheses, but it necessitates consideration of recycling strategies to reclaim the biological templating molecules for use in subsequent syntheses. Some effort will have to be focused on post-synthetic fixation of the NP superstructures (e.g., in epoxy or silica) and subsequent release or removal of the biological templating agents. These are not insurmountable tasks, however, and potential fears of scalability and cost should not deter those interested in contributing to this exciting field where much fundamental exploration and discovery remains.

Acknowledgements

S.M.-P., Y.Z., and S.C.B. contributed equally to the writing of this manuscript. The authors thank the University of Pittsburgh and the National Science Foundation (DMR 1904960, N.L.R.) for generously funding this work. S.M.-P. and S.C.B. both acknowledge support from the University of Pittsburgh Dietrich School of Arts and Sciences through Andrew W. Mellon and Arts and Sciences graduate research fellowships, respectively.

Conflict of Interest

The authors declare no conflict of interest.

Keywords

chiral nanoparticles, helical nanoparticle assembly, nanomaterials, plasmonic chiroptical activity

Received: September 11, 2019

Revised: October 12, 2019

Published online:

- [1] N. Fujii, T. Saito, *Chem. Rec.* **2004**, 4, 267.
- [2] J. B. Pendry, *Science* **2004**, 306, 1353.
- [3] J. K. Gansel, M. Thiel, M. S. Rill, M. Decker, K. Bade, V. Saile, G. von Freymann, S. Linden, M. Wegener, *Science* **2009**, 325, 1513.
- [4] M. Decker, M. W. Klein, M. Wegener, S. Linden, *Opt. Lett.* **2007**, 32, 856.
- [5] D. R. Smith, J. B. Pendry, M. C. K. Wiltshire, *Science* **2004**, 305, 788.
- [6] A. V. Rogacheva, V. A. Fedotov, A. S. Schwanecke, N. I. Zheludev, *Phys. Rev. Lett.* **2006**, 97, 177401.
- [7] J. B. Pendry, *Phys. Rev. Lett.* **2000**, 85, 3966.
- [8] Y. Zhu, L. Xu, W. Ma, Z. Xu, H. Kuang, L. Wang, C. Xu, *Chem. Commun.* **2012**, 48, 11889.
- [9] E. Plum, J. Zhou, J. Dong, V. A. Fedotov, T. Koschny, C. M. Soukoulis, N. I. Zheludev, *Phys. Rev. B* **2009**, 79, 035407.
- [10] S. Zhang, Y.-S. Park, J. Li, X. Lu, W. Zhang, X. Zhang, *Phys. Rev. Lett.* **2009**, 102, 023901.
- [11] J. Kumar, H. Eraña, E. López-Martínez, N. Claes, V. F. Martín, D. M. Solís, S. Bals, A. L. Cortajarena, J. Castilla, L. M. Liz-Marzán, *Proc. Natl. Acad. Sci. USA* **2018**, 115, 3225.
- [12] J. Sivaguru, T. Poon, R. Franz, S. Jockusch, W. Adam, N. J. Turro, *J. Am. Chem. Soc.* **2004**, 126, 10816.
- [13] N. Shukla, M. A. Bartel, A. J. Gellman, *J. Am. Chem. Soc.* **2010**, 132, 8575.
- [14] S. A. Maier, *Plasmonics: Fundamentals and Applications*, Springer US, New York **2007**.
- [15] K. L. Kelly, E. Coronado, L. L. Zhao, G. C. Schatz, *J. Phys. Chem. B* **2003**, 107, 668.
- [16] K.-S. Lee, M. A. El-Sayed, *J. Phys. Chem. B* **2006**, 110, 19220.
- [17] A. P. Alivisatos, *Science* **1996**, 271, 933.
- [18] Z. Fan, A. O. Govorov, *J. Phys. Chem. C* **2011**, 115, 13254.
- [19] A. Ben-Moshe, B. M. Maoz, A. O. Govorov, G. Markovich, *Chem. Soc. Rev.* **2013**, 42, 7028.
- [20] N. Berova, L. D. Bari, G. Pescitelli, *Chem. Soc. Rev.* **2007**, 36, 914.
- [21] A. Guerrero-Martínez, B. Auguie, J. L. Alonso-Gómez, Z. Džolić, S. Gómez-Graña, M. Žinić, M. M. Cid, L. M. Liz-Marzán, *Angew. Chem., Int. Ed.* **2011**, 50, 5499.

- [22] A. D. Merg, J. C. Boatz, A. Mandal, G. Zhao, S. Mokashi-Punekar, C. Liu, X. Wang, P. Zhang, P. C. A. van der Wel, N. L. Rosi, *J. Am. Chem. Soc.* **2016**, 138, 13655.
- [23] Z. Fan, A. O. Govorov, *Nano Lett.* **2010**, 10, 2580.
- [24] S. L. Burkett, S. Mann, *Chem. Commun.* **1996**, 321.
- [25] E. D. Sone, E. R. Zubarev, S. I. Stupp, *Angew. Chem., Int. Ed.* **2002**, 41, 1705.
- [26] X. Fu, Y. Wang, L. Huang, Y. Sha, L. Gui, L. Lai, Y. Tang, *Adv. Mater.* **2003**, 15, 902.
- [27] C.-L. Chen, P. Zhang, N. L. Rosi, *J. Am. Chem. Soc.* **2008**, 130, 13555.
- [28] J. Sharma, R. Chhabra, A. Cheng, J. Brownell, Y. Liu, H. Yan, *Science* **2009**, 323, 112.
- [29] S. A. Claridge, S. L. Goh, J. M. J. Fréchet, S. C. Williams, C. M. Micheel, A. P. Alivisatos, *Chem. Mater.* **2005**, 17, 1628.
- [30] A. J. Mastroianni, S. A. Claridge, A. P. Alivisatos, *J. Am. Chem. Soc.* **2009**, 131, 8455.
- [31] W. Chen, A. Bian, A. Agarwal, L. Liu, H. Shen, L. Wang, C. Xu, N. A. Kotov, *Nano Lett.* **2009**, 9, 2153.
- [32] A. O. Govorov, Y. K. Gun'ko, J. M. Slocik, V. A. Gérard, Z. Fan, R. R. Naik, *J. Mater. Chem.* **2011**, 21, 16806.
- [33] Y. Wang, Q. Wang, H. Sun, W. Zhang, G. Chen, Y. Wang, X. Shen, Y. Han, X. Lu, H. Chen, *J. Am. Chem. Soc.* **2011**, 133, 20060.
- [34] X. Shen, C. Song, J. Wang, D. Shi, Z. Wang, N. Liu, B. Ding, *J. Am. Chem. Soc.* **2012**, 134, 146.
- [35] A. Kuzyk, R. Schreiber, Z. Fan, G. Pardatscher, E.-M. Roller, A. Högele, F. C. Simmel, A. O. Govorov, T. Liedl, *Nature* **2012**, 483, 311.
- [36] C. Song, M. G. Blaber, G. Zhao, P. Zhang, H. C. Fry, G. C. Schatz, N. L. Rosi, *Nano Lett.* **2013**, 13, 3256.
- [37] G. Singh, H. Chan, A. Baskin, E. Gelman, N. Reprnin, P. Král, R. Klajn, *Science* **2014**, 345, 1149.
- [38] J. Yeom, B. Yeom, H. Chan, K. W. Smith, S. Dominguez-Medina, J. H. Bahng, G. Zhao, W.-S. Chang, S.-J. Chang, A. Chuvilin, D. Melnikau, A. L. Rogach, P. Zhang, S. Link, P. Král, N. A. Kotov, *Nat. Mater.* **2015**, 14, 66.
- [39] M. J. Urban, P. K. Dutta, P. Wang, X. Duan, X. Shen, B. Ding, Y. Ke, N. Liu, *J. Am. Chem. Soc.* **2016**, 138, 5495.
- [40] X. Lan, T. Liu, Z. Wang, A. O. Govorov, H. Yan, Y. Liu, *J. Am. Chem. Soc.* **2018**, 140, 11763.
- [41] F. Leroux, M. Gysemans, S. Bals, K. J. Batenburg, J. Snauwaert, T. Verbiest, C. Van Haesendonck, G. Van Tendeloo, *Adv. Mater.* **2010**, 22, 2193.
- [42] C. Song, G. Zhao, P. Zhang, N. L. Rosi, *J. Am. Chem. Soc.* **2010**, 132, 14033.
- [43] C.-L. Chen, N. L. Rosi, *J. Am. Chem. Soc.* **2010**, 132, 6902.
- [44] A. D. Merg, J. Slocik, M. G. Blaber, G. C. Schatz, R. Naik, N. L. Rosi, *Langmuir* **2015**, 31, 9492.
- [45] J. M. Slocik, M. O. Stone, R. R. Naik, *Small* **2005**, 1, 1048.
- [46] C. Zhang, C. Song, H. C. Fry, N. L. Rosi, *Chem. – Eur. J.* **2014**, 20, 941.
- [47] S. Mokashi-Punekar, A. D. Merg, N. L. Rosi, *J. Am. Chem. Soc.* **2017**, 139, 15043.
- [48] S. Mokashi-Punekar, N. L. Rosi, *Part. Part. Syst. Charact.* **2019**, 36, 1800504.
- [49] E. S. Kang, Y.-T. Kim, Y.-S. Ko, N. H. Kim, G. Cho, Y. H. Huh, J.-H. Kim, J. Nam, T. T. Thach, D. Youn, Y. D. Kim, W. S. Yun, W. F. DeGrado, S. Y. Kim, P. T. Hammond, J. Lee, Y.-U. Kwon, D.-H. Ha, Y. H. Kim, *ACS Nano* **2018**, 12, 6554.
- [50] P. W. K. Rothmund, *Nature* **2006**, 440, 297.
- [51] M. R. Jones, N. C. Seeman, C. A. Mirkin, *Science* **2015**, 347, 1260901.
- [52] C. Shen, X. Lan, C. Zhu, W. Zhang, L. Wang, Q. Wang, *Adv. Mater.* **2017**, 29, 1606533.
- [53] X. Lan, X. Lu, C. Shen, Y. Ke, W. Ni, Q. Wang, *J. Am. Chem. Soc.* **2015**, 137, 457.
- [54] A. Ceconello, J. S. Kahn, C.-H. Lu, L. Khosravi Khorashad, A. O. Govorov, I. Willner, *J. Am. Chem. Soc.* **2016**, 138, 9895.
- [55] E. D. Sone, E. R. Zubarev, S. I. Stupp, *Small* **2005**, 1, 694.
- [56] Y. Zhou, Q. Ji, M. Masuda, S. Kamiya, T. Shimizu, *Chem. Mater.* **2006**, 18, 403.
- [57] M. Nakagawa, T. Kawai, *J. Am. Chem. Soc.* **2018**, 140, 4991.
- [58] J. George, S. Kar, E. S. Anupriya, S. M. Somasundaran, A. D. Das, C. Sissa, A. Painelli, K. G. Thomas, *ACS Nano* **2019**, 13, 4392.
- [59] S.-H. Yu, H. Cölfen, K. Tauer, M. Antonietti, *Nat. Mater.* **2005**, 4, 51.
- [60] H. S. Oh, S. Liu, H. Jee, A. Baev, M. T. Swihart, P. N. Prasad, *J. Am. Chem. Soc.* **2010**, 132, 17346.
- [61] S. H. Jung, J. Jeon, H. Kim, J. Jaworski, J. H. Jung, *J. Am. Chem. Soc.* **2014**, 136, 6446.
- [62] X. Lu, D.-p. Song, A. Ribbe, J. J. Watkins, *Macromolecules* **2017**, 50, 5293.
- [63] M. Mitov, C. Bourgerette, F. d. Guerville, *J. Phys.: Condens. Matter* **2004**, 16, S1981.
- [64] L. Cseh, X. Mang, X. Zeng, F. Liu, G. H. Mehl, G. Ungar, G. Siligardi, *J. Am. Chem. Soc.* **2015**, 137, 12736.
- [65] G. Chu, X. Wang, T. Chen, J. Gao, F. Gai, Y. Wang, Y. Xu, *ACS Appl. Mater. Interfaces* **2015**, 7, 11863.
- [66] J. Majoinen, J. Hassinen, J. S. Haataja, H. T. Rekola, E. Kontturi, M. A. Kostianen, R. H. A. Ras, P. Törmä, O. Ikkala, *Adv. Mater.* **2016**, 28, 5262.
- [67] R.-Y. Wang, H. Wang, X. Wu, Y. Ji, P. Wang, Y. Qu, T.-S. Chung, *Soft Matter* **2011**, 7, 8370.
- [68] R. Tamoto, S. Lecomte, S. Si, S. Moldovan, O. Ersen, M.-H. Delville, R. Oda, *J. Phys. Chem. C* **2012**, 116, 23143.
- [69] J. Cheng, G. Le Saux, J. Gao, T. Buffeteau, Y. Battie, P. Barois, V. Ponsinet, M.-H. Delville, O. Ersen, E. Pouget, R. Oda, *ACS Nano* **2017**, 11, 3806.
- [70] L. Jiang, J. W. J. de Folter, J. Huang, A. P. Philipse, W. K. Kegel, A. V. Petukhov, *Angew. Chem., Int. Ed.* **2013**, 52, 3364.
- [71] P. Bai, S. Yang, W. Bao, J. Kao, K. Thorkelsson, M. Salmeron, X. Zhang, T. Xu, *Nano Lett.* **2017**, 17, 6847.
- [72] S. Srivastava, A. Santos, K. Critchley, K.-S. Kim, P. Podsiadlo, K. Sun, J. Lee, C. Xu, G. D. Lilly, S. C. Glotzer, N. A. Kotov, *Science* **2010**, 327, 1355.
- [73] G. D. Lilly, A. Agarwal, S. Srivastava, N. A. Kotov, *Small* **2011**, 7, 2004.
- [74] Y. Zhou, R. L. Marson, G. van Anders, J. Zhu, G. Ma, P. Ercius, K. Sun, B. Yeom, S. C. Glotzer, N. A. Kotov, *ACS Nano* **2016**, 10, 3248.
- [75] S. Jana, M. de Frutos, P. Davidson, B. Abécassis, *Sci. Adv.* **2017**, 3, e1701483.
- [76] A. R. A. Palmans, J. A. J. M. Vekemans, E. E. Havinga, E. W. Meijer, *Angew. Chem., Int. Ed. Engl.* **1997**, 36, 2648.